

# Synthesis of naproxen thiadiazole urea hybrids and determination of their anti-melanoma, anti-migration, tyrosinase inhibitory activity, and molecular docking studies

Belma Zengin Kurt<sup>a,\*</sup>, Özlem Altundağ<sup>b</sup>, Mustafa Gökçe<sup>c</sup>, Ummuhan Cakmak<sup>d</sup>, Fulya Oz Tuncay<sup>d</sup>, Yakup Kolcuoğlu<sup>d</sup>, Ayşenur Günaydın Akyıldız<sup>e</sup>, Atilla Akdemir<sup>f</sup>, Dilek Öztürk Civelek<sup>c</sup>, Fatih Sönmez<sup>g</sup>

<sup>a</sup> Bezmialem Vakif University, Faculty of Pharmacy, Department of Pharmaceutical Chemistry, 34093, Istanbul, Türkiye

<sup>b</sup> Bezmialem Vakif University, Faculty of Pharmacy, 34093, Istanbul, Türkiye

<sup>c</sup> Bezmialem Vakif University, Faculty of Pharmacy, Department of Pharmacology, 34093, Istanbul, Türkiye

<sup>d</sup> Karadeniz Technical University, Faculty of Science, Department of Chemistry, 61080, Trabzon, Türkiye

<sup>e</sup> Bezmialem Vakif University, Faculty of Pharmacy, Department of Pharmaceutical Toxicology, 34093, Istanbul, Türkiye

<sup>f</sup> Istinye University, Faculty of Pharmacy, Department of Pharmacology, 34396, Istanbul, Türkiye

<sup>g</sup> Sakarya University of Applied Sciences, Pamukova Vocational School, 54055, Sakarya, Türkiye

## ARTICLE INFO

### Keywords:

Naproxen Urea  
Thiadiazole ring  
Tyrosinase inhibition  
Cytotoxicity  
Anti-migration effect  
Molecular docking

## ABSTRACT

Novel sixteen naproxen urea compounds were synthesized bearing the thiadiazole ring. Their inhibitory activities against tyrosinase were investigated. **3o** was discovered to be the most potent inhibitor of tyrosinase, with an IC<sub>50</sub> value of 35.0 μM. The kinetic parameters were used to determine the type of enzyme inhibition. The results showed that **3o** was an uncompetitive inhibitor with the K<sub>i</sub> value of 62.2 μM. Additionally, the cytotoxic effects of the synthesized compounds on melanoma (B16F10), mouse embryonic (3T3) and the healthy 3T3 cell lines were also investigated. According to the cytotoxicity results, **3e** (IC<sub>50</sub>= 2.17 μM) showed the highest cytotoxicity on the B16F10 cells. Furthermore, the effects of selected compounds on the migration rate of melanoma cells were investigated. In addition, molecular modeling studies were also performed and the results showed the possible interactions between the uncompetitive inhibitor **3o** with the Tyrosinase-L-Tyrosine enzyme substrate complex.

## 1. Introduction

Tyrosinase (EC 1.14.18.1, TYR) is a type III copper-containing oxidoreductase enzyme. This enzyme catalyses some reactions such as the hydroxylation of monophenols to *o*-diphenols or the oxidation of *o*-diphenols to *o*-quinones [1,2]. On the other hand, tyrosinase can control dopamine toxicity and thus it affects the induction and development process of many important neurodegenerative diseases such as Parkinson's disease [3]. Tyrosinase is also a key enzyme in melanin biosynthesis, which plays an important role in many physiological and pathological pathways [4]. When *L*-tyrosine is used as a substrate, the product of the tyrosinase-catalysed reaction is dopaquinone, which can easily convert to melanin [5]. Recent studies have shown that tyrosinase activity is closely related to the incidence of melanoma [6].

Melanin is an essential biopolymer responsible for mammal skin, eye and hair colour. Melanin is produced in melanocytes by a process called melanogenesis, which is restricted to special organelles called melanosomes [7]. This melanin produced is one of the mechanisms that protects the skin against ultraviolet (UV) damage and removes reactive oxygen species (ROS) [8,9]. Abnormal levels of melanin are associated with a variety of pathologies, such as hyperpigmentation, melanoma, or ochronosis-related dermatological disorders that occur in alkaptonuria [3,10,11]. Melanoma is characterized by the disorganization of melanocytes that produce melanin by keratinocytes in the epidermal skin. This irregularity causes the uncontrolled proliferation of melanocytes, so a high melanin content is observed in most cases of melanoma [10–13].

Therefore, inhibition of the tyrosinase enzyme responsible for

\* Corresponding author.

E-mail address: [bzengin@bezmialem.edu.tr](mailto:bzengin@bezmialem.edu.tr) (B. Zengin Kurt).

<https://doi.org/10.1016/j.molstruc.2023.136618>

Received 28 July 2023; Received in revised form 28 August 2023; Accepted 8 September 2023

Available online 8 September 2023

0022-2860/© 2023 Elsevier B.V. All rights reserved.

melanin biosynthesis can prevent an abnormal increase in melanin levels and related diseases [14]. Mushroom tyrosinase is an accessible, commercially available enzyme due to its solubility and it is a widely used model to identify tyrosinase inhibitors. In addition, mushroom tyrosinase inhibitors show increased activity in murine and human tyrosinases in general [15]. This provides a good feature for the discovery of new inhibitors in the mushroom tyrosinase model [16].

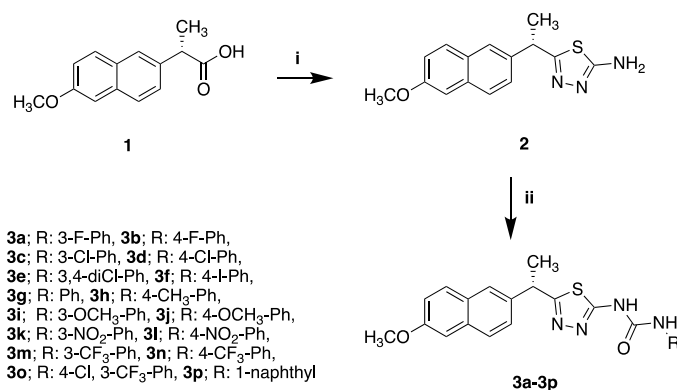
Thiosemicarbazones constitute a versatile class of ligands and have numerous pharmacological and biological properties such as antimicrobial, antimicrobial and anticancer agents [17–21]. In recent years, thiosemicarbazone derivatives have also received great attention as tyrosinase inhibitors [22]. Its derivatives including the aromatic ring mimic natural tyrosinase substrates (*L*-tyrosine and *L*-dopa etc.). Tyrosinase inhibitors can generally both interact hydrophobically with the tyrosinase cavity through van der Waals interactions, and the electronegative sulphur and nitrogen atoms of the thiourea moiety can enhance the coordination abilities of the ligand and act as chelators of copper ions in the active site of the enzyme [22]. The structures of some known tyrosinase derivatives are given in Fig. 1. The thiadiazole ring is a structural isomer of the thiosemicarbazide structure and has a wide range of biological activities [23]. However, researches about this structure as tyrosinase inhibitors are not sufficiently included in the literature.

Since the antiproliferative effect of Sulindac was first observed in reducing colon adenomas in 1983, researches have been conducted to evaluate the anticancer potential of the non-steroidal anti-inflammatory drugs (NSAIDs) [24–26]. In this study, naproxen, one of the NSAIDs, was chosen as the main scaffold. Its derivative bearing thiadiazole amine was synthesized from the thiosemicarbazone skeleton and converted to its cyclic isomer, and then urea derivatives were obtained by reaction with phenyl isocyanates. Furthermore, the tyrosinase inhibitory activities and anti-melanoma properties of the synthesized compounds were investigated. In addition, the inhibition kinetic parameters and mechanisms were evaluated and enzyme-ligand interactions were demonstrated by molecular modeling studies.

## 2. Result and discussion

### 2.1. Chemistry

The novel Naproxen thiadiazole-urea hybrids were synthesized as shown in Scheme 1. Naproxen (1, (*S*)-(+)-2-(6-Methoxy-2-naphthyl)propionic acid) was reacted with thiosemicarbazide at 75°C for 1 hour to give (*S*)-5-(1-(6-methoxynaphthalen-2-yl)ethyl)-1,3,4-thiadiazol-2-



**Scheme 1.** Synthesis of novel Naproxen thiadiazole-urea derivatives. Reaction condition; i) 1) POCl<sub>3</sub>, Thiosemicarbazide, 75°C, 1 h, 2) NaOH, 50 %; ii) DMF, DBU, Phenylisocyanate derivatives, 60 °C, 18 h.

amine (2). The carboxylic acid moiety converts to the acyl chloride with POCl<sub>3</sub> and then it reacts with the NH<sub>2</sub> of thiosemicarbazide. The ring closure occurs with the following reaction tautomer of the formed structure and POCl<sub>3</sub>. After that, urea derivatives (**3a-3p**) were obtained from the reaction of naproxen thiadiazole amine (2) and various phenyl isocyanate derivatives in DMF with the DBU as a catalyst. Attempts were made with different bases for this step, but the yield obtained with DBU was not achieved. By removing the proton of the amino group at DBU, it enables the NH<sub>2</sub> group to attack the isocyanate structure more easily.

From the <sup>1</sup>H NMR spectra of compound 2, the signals for NH<sub>2</sub> protons were observed between at 7.77–7.86 ppm and the signals for OH proton of carboxylic acid disappeared. The peak in the 180 ppm belonging to carboxylic acid disappeared, and at 169.5 ppm, the signal of the carbon atom of the thiadiazole ring was observed. From the <sup>1</sup>H NMR spectra of compounds **3a-3p**; the signals for aromatic protons were observed between 6.80 and 8.56 ppm, while aliphatic proton signals observed about at 1.77–4.70 ppm. The signal of the -NH protons were observed in the range of 9.11–11.15 ppm. From the <sup>13</sup>C NMR spectra, the signals of the aliphatic and aromatic carbons were observed at 21–55.6 ppm and 105.0–160.0 ppm, respectively. Among these peaks, the urea carbon signals were observed around 157 ppm, while the carbon (adjacent to NH) of the thiadiazole ring was observed in the range of 158–165 ppm.

### 2.2. Tyrosinase inhibitory activity and structure activities relationships

The IC<sub>50</sub> values (μM) of **3a-p** against tyrosinase are given in Table 1.

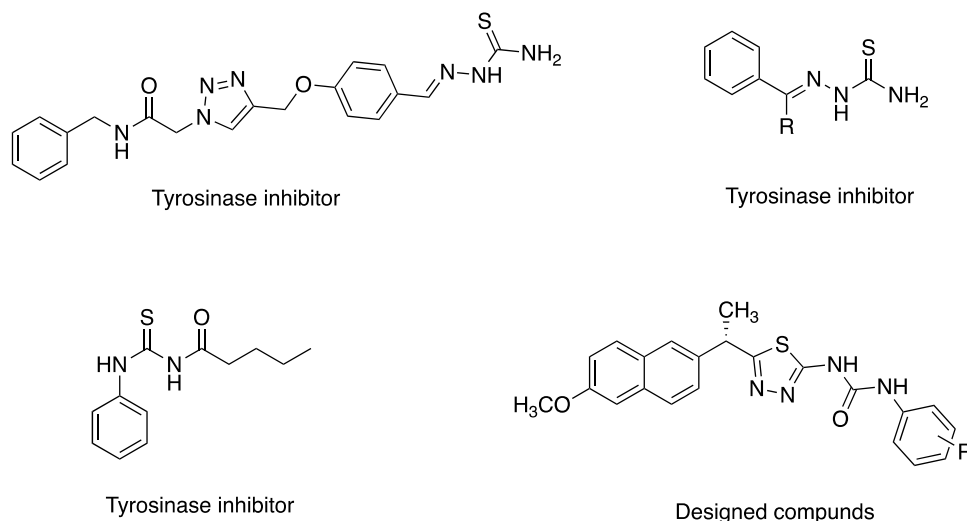
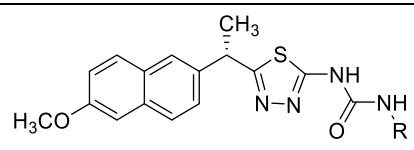


**Fig. 1.** The structure of known thiosemicarbazide derivatives as tyrosinase inhibitors.

**Table 1**

The tyrosinase inhibitory activity of novel Naproxen thiazazole-urea derivatives.



Comp.	R	IC <sub>50</sub> , μM	Max. Inhibition %	[I], μM
<b>3a</b>	3-F-Ph	410.0±1.6	53.8±0.6	500
<b>3b</b>	4-F-Ph	50.0±0.3	72.0±1.3	250
<b>3c</b>	3-Cl-Ph	78.0±1.0	68.7±0.7	250
<b>3d</b>	4-Cl-Ph	80.0±1.1	72.6±1.0	500
<b>3e</b>	3,4-diCl-Ph	225.0±1.3	53.3±0.8	250
<b>3f</b>	4-I-Ph	175.0±1.0	55.1±0.8	250
<b>3g</b>	Ph	>250	43.0±0.6	250
<b>3h</b>	4-CH <sub>3</sub> -Ph	>500	40.2±0.5	500
<b>3i</b>	3OCH <sub>3</sub> -Ph	>500	41.3±0.6	500
<b>3j</b>	4OCH <sub>3</sub> -Ph	>500	32.4±0.4	500
<b>3k</b>	3-NO <sub>2</sub> -Ph	>125	26.1±0.3	125
<b>3l</b>	4-NO <sub>2</sub> -Ph	>250	29.7±0.4	250
<b>3m</b>	3-CF <sub>3</sub> -Ph	220.0±1.3	53.3±0.7	250
<b>3n</b>	4-CF <sub>3</sub> -Ph	80.0±0.5	65.8±0.8	250
<b>3o</b>	4-Cl, 3-CF <sub>3</sub> -Ph	35.0±0.6	79.2±1.0	250
<b>3p</b>	1-naphthyl	130.0±1.0	53.9±0.7	200
Kojic acid		200.0±1.1	85.7±0.7	1000

All synthesized compounds (**3a-p**) inhibited tyrosinase with the IC<sub>50</sub> values ranging from 35.0 μM to >500 μM. Among them, **3o** showed the strongest tyrosinase inhibitory activity with the IC<sub>50</sub> value of 35.0 μM which is almost 6-fold higher than kojic acid (IC<sub>50</sub> = 200.0 μM) which was used as a standard. Moreover, six compounds (**3b-3d**, **3f**, **3n**, and **3p**) showed better inhibitory activity against tyrosinase compared to kojic acid.

In addition, the following structure-activity relationship can be inferred from Table 1;

Generally, the compounds bearing halogens and/or electron withdrawing groups (F, Cl, I, CF<sub>3</sub>, NO<sub>2</sub>) at the phenyl ring have stronger inhibitory activity against tyrosinase than the compounds including electron donating groups (OCH<sub>3</sub>, CH<sub>3</sub>) at the phenyl ring (Fig. 2).

Moving the -F and -CF<sub>3</sub> substituents at the phenyl ring from *meta*- to *para*- position increased the tyrosinase inhibition (compared **3a** (R=3-F-Ph, IC<sub>50</sub> = 410.0 μM) with **3b** (R=4-F-Ph, IC<sub>50</sub> = 50.0 μM); compared **3m** (R=3-CF<sub>3</sub>-Ph, IC<sub>50</sub> = 220.0 μM) with **3n** (R=4-CF<sub>3</sub>-Ph, IC<sub>50</sub> = 80.0 μM)). On the other hand, moving the OCH<sub>3</sub>- and -Cl substituents at the phenyl ring from *meta*- to *para*- position did not significantly affect the tyrosinase inhibitory activity (compared **3i** (R=3-OCH<sub>3</sub>-Ph, IC<sub>50</sub> = >500 μM) with **3j** (R=4-OCH<sub>3</sub>-Ph, IC<sub>50</sub> = >500.0 μM); compared **3c** (R=3-Cl-Ph, IC<sub>50</sub> = 78.0 μM) with **3d** (R=4-Cl-Ph, IC<sub>50</sub> = 80.0 μM)).

Binding the second -Cl to the phenyl ring decreased the tyrosinase inhibitions (compared **3c** (R=3-Cl-Ph, IC<sub>50</sub> = 78.0 μM) and **3d** (R=4-Cl-Ph, IC<sub>50</sub> = 80.0 μM) with **3e** (R=3,4-diCl-Ph, IC<sub>50</sub> = 225.0 μM)). On the other hand, binding the -Cl to the *para*- position at the phenyl ring of compound **3o** (R=3-CF<sub>3</sub>-Ph) raised the inhibitory activity against

tyrosinase (compared **3m** (R=3-CF<sub>3</sub>-Ph, IC<sub>50</sub> = 220.0 μM) with **3o** (R=4-Cl, 3-CF<sub>3</sub>-Ph, IC<sub>50</sub> = 35.0 μM)).

Compound **3p** (R=1-naphthyl, IC<sub>50</sub> = 130.0 μM), containing a naphthyl moiety, showed higher inhibitory activity against tyrosinase than compound **3g** (R=Ph, IC<sub>50</sub> = >250.0 μM), containing a non-substituted phenyl moiety.

The growing size and polarizability of the halogen series at the *para*-position of the phenyl ring notably decreased tyrosinase inhibition (for size and polarizability, I > Cl > F; for inhibitory activity, **3f** (R=4-I-Ph, IC<sub>50</sub> = 175.0 μM) < **3d** (R=4-Cl-Ph, IC<sub>50</sub> = 80.0 μM) < **3b** (R=4-F-Ph, IC<sub>50</sub> = 50.0 μM)).

Compounds **3h-3j** (bearing methyl or methoxy as an electron-donating group) had the lowest inhibitory activity against tyrosinase among all synthesized compounds.

### 2.3. Kinetic studies of mushroom tyrosinase inhibition

In order to determine the inhibitory effects of newly synthesized Naproxen thiazazole-urea derivatives (**3a-3p**) on mushroom tyrosinase, their solutions at different concentrations were prepared by dissolving the compounds in DMF. Since DMF is included in the enzyme activity protocol, a 2 % concentration did not have a negative effect on the enzyme. The IC<sub>50</sub> value could not be calculated for **3g** to **3l** molecules. The decrease in the solubility of the molecules dissolved in the organic solvent in the aqueous medium used while determining the enzyme activity was effective in this process. The most active compound **3o** was chosen to evaluate the inhibition type of these substances. The inhibition type of the selected molecule was determined by drawing the

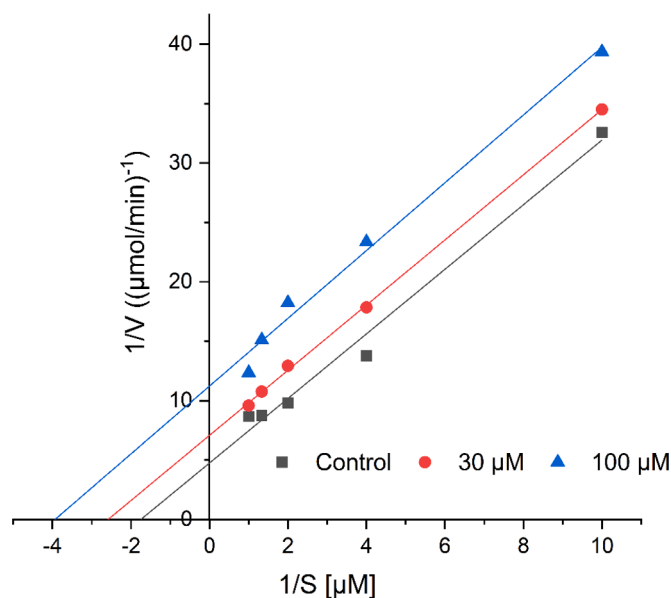
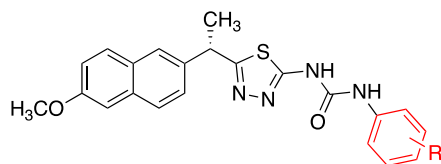


Fig. 3. Lineweaver-Burk plots for the inhibition of tyrosinase in the presence of **3o**.



**Inhibitory activity; 3a-3f** (R=Halogens: F, Cl, I), **3k-3o** (R= Electron withdrawing group: NO<sub>2</sub>, CF<sub>3</sub>) > **3h-3i** (R= Electron donating group: CH<sub>3</sub>, OCH<sub>3</sub>)

Fig. 2. The general structure of synthesized compounds for SAR.

Lineweaver-Burk graph (Fig. 3). For this purpose, the enzyme activity was determined in the presence and absence of the inhibitor by selecting values in the concentration range that causes 25–75 % inhibition, which is used to determine the IC<sub>50</sub> value. From the graph obtained, the inhibition type was determined as uncompetitive and the K<sub>i</sub> value was calculated as 62.2 μM (Table 2).

#### 2.4. Cytotoxicity

The murine melanoma cell line (B16F10) and mouse embryonic cell line (3T3) were used to evaluate the cytotoxic activity of Naproxen thiadiazole-urea derivatives (**3a–3p**) according to the MTT assay (Table 3). 12 of the synthesized compounds showed higher cytotoxicity against B16F10 cancer cell lines compared to naproxen. The most cytotoxic compound on B16F10 was **3e** (IC<sub>50</sub>=2.17 μM). Moreover, the cytotoxic activities of **3f** (IC<sub>50</sub>=2.62 μM), **3g** (IC<sub>50</sub>=3.43 μM), **3h** (IC<sub>50</sub>=4.68 μM), **3j** (IC<sub>50</sub>=4.15 μM), **3l** (IC<sub>50</sub>=4.15 μM), **3m** (IC<sub>50</sub>=5.96 μM), **3n** (IC<sub>50</sub>=7.41 μM), **3o** (IC<sub>50</sub>=9.57 μM), and **3p** (IC<sub>50</sub>=5.09 μM) were also high against B16F10 cells. All the compounds showed higher cytotoxicity against the healthy 3T3 cell line compared to naproxen. Some of the compounds showed a strong cytotoxic effect on cancer cells, the other part showed a high cytotoxic effect on healthy cells. As seen from the selective index in Table 3, **3e–3m** showed better cytotoxicity on cancer cells, while **3a–3d** showed higher cytotoxicity on healthy cell lines. **3n–3p** showed cytotoxicity close to cancer and healthy cell lines. Naproxen showed higher selectivity compared to the synthesized compounds, but its cytotoxic effect on cancer cells was still lower than other substances. These results showed that some of the synthesized naproxen thiadiazole-urea derivatives gained cytotoxic and potentially anticancer properties against cancer cell lines compared to naproxen, used as the main skeleton. In addition, their anti-tyrosinase activity is also promising for use in melanomas.

#### 2.5. Cell migration

Among the synthesized compounds, two compounds with high enzyme inhibition (**3n**, **3o**) and two compounds with high cytotoxic effect (**3e**, **3g**) were selected, and the anti-migration effects of these selected compounds were investigated. **3n** and **3o** inhibited the migration of the B16F10 melanoma cells after 24 h treatment compared to the control group while **3e** and **3g** did not show significant effects (Fig. 4). These results show that **3n** and **3o** may have potential anticancer properties inhibiting cell migration against melanoma cancer cells in addition to their cytotoxic and anti-tyrosinase activities. According to these results, it has been shown that the anti-migration properties of compounds with better enzyme inhibition are higher. There are some studies showing that migration and tyrosinase activity increase together [27–29]. In these studies, it is seen that migration increases with the induction of tyrosinase activity. According to our results, compounds that provide tyrosinase inhibition also prevent cell migration.

#### 2.6. Molecular modeling studies

A homology model of *Agaricus bisporus* Tyrosinase (UniProt entry: C7FF04) was constructed based on the crystal structure of *Aspergillus oryzae* Tyrosinase in complex with *L*-tyrosine (PDB entry: 6JU9). Compound **3o** was docked into the active site of the newly constructed

**Table 2**

Kinetic parameters for the compounds **3o** against mushroom tyrosinase inhibition assay.

3o (μM)	K <sub>m</sub> (mM)	V <sub>max</sub> (μmol/min)	Inhibition types	K <sub>i</sub> (μM)
Control	0.57	0.21	Uncompetitive	62.2
30	0.39	0.14		
100	0.25	0.09		

**Table 3**

IC<sub>50</sub> values of the cytotoxicity of synthesized molecules at B16F10 and 3T3 cell line.

Compound	R	B16F10, IC <sub>50</sub> (μM)*	3T3, IC <sub>50</sub> (μM)	SI**
<b>3a</b>	3-F-Ph	125.61±32.47	17.28±2.61	0.13
<b>3b</b>	4-F-Ph	165.19±25.04	8.48±0.69	0.051
<b>3c</b>	3-Cl-Ph	71.33±22.91	5.10±0.36	0.071
<b>3d</b>	4-Cl-Ph	92.65±25.05	6.47±0.59	0.069
<b>3e</b>	3,4-diCl-Ph	2.17±0.45	9.57±1.25	4.41
<b>3f</b>	4-I-Ph	2.62±0.72	6.28±0.33	0.1
<b>3g</b>	Ph	3.43±0.81	14.67±1.08	4.27
<b>3h</b>	4-CH <sub>3</sub> -Ph	4.68±1.16	8.39±0.86	1.79
<b>3i</b>	3OCH <sub>3</sub> -Ph	32.51±6.99	34.56±5.75	1.06
<b>3j</b>	4OCH <sub>3</sub> -Ph	7.67±2.54	12.62±0.77	1.64
<b>3k</b>	3-NO <sub>2</sub> -Ph	18.66±4.53	20.83±3.00	1.12
<b>3l</b>	4-NO <sub>2</sub> -Ph	4.15±0.53	13.36±1.66	3.22
<b>3m</b>	3-CF <sub>3</sub> -Ph	5.96±1.25	9.04±1.45	1.51
<b>3n</b>	4-CF <sub>3</sub> -Ph	7.41±1.66	5.25±0.33	0.70
<b>3o</b>	4-Cl, 3-CF <sub>3</sub> -Ph	9.57±2.23	3.99±0.48	0.41
<b>3p</b>	1-naphthyl	5.09±1.35	4.62±0.35	0.90
<b>Naproxen</b>	-	33.48±8.90	222.74±50.75	6.65

\* The cell viability was represented as a percentage (%) relative to untreated cells as a control.

\*\* Selectivity Index (3T3/B16F10)

homology model with *L*-Tyrosine bound to investigate potential interactions between the uncompetitive inhibitor **3o** and the *L*-Tyrosine-Tyrosinase complex. The docked pose showed the presence of an aromatic Hydrogen bond with the side chain of Gln207 and π-π stackings with the side chain of His244 (Fig. 5A and B). **3o** formed direct Hydrogen bonds with the substrate *L*-Tyrosine. The RMSD of the ligand increased during the 250 ns MD simulation (Fig. 5C). However, **3o** was able to form interactions with the enzyme-substrate complex throughout the simulation (Fig. 5D). **3o** formed direct Hydrogen bonds with Asn81 and the substrate *L*-Tyrosinase and water-mediated Hydrogen bonds with Asn81 and Asn209. In addition, π-π stackings were formed with Tyr82 and His244.

The MM-GBSA binding energy was calculated for the course of the 250 ns MD simulation and the average value was -64.9185 +/-8.90 kcal/mol with a range of -93.4659 to -41.3480 kcal/mol (Fig. 5E).

### 3. Conclusion

In conclusion, sixteen novel Naproxen urea derivatives bearing the thiadiazole ring were synthesized. Most of these compounds showed inhibitory activity in the micromolar range against tyrosinase. Compound **3o** exhibited the strongest inhibitory activity against tyrosinase with IC<sub>50</sub> values of 35.0 μM. The inhibition type of **3o** was determined as uncompetitive and the K<sub>i</sub> value was calculated as 62.2 μM. **3e** (IC<sub>50</sub>=2.17 μM) showed the highest anti-melanoma activity with the highest cytotoxicity on B16F10 cells, but did not present anti-migratory effects. However, **3o** showed dose-dependent anti-migratory effect on B16F10 cells. This demonstrated that compounds with superior enzyme inhibition were more effective at inhibiting cell migration. Molecular modeling studies suggested possible interactions between the uncompetitive inhibitor **3o** with the Tyrosinase-*L*-Tyrosine enzyme-substrate complex.

As a result of all these studies, the **3o** showed remarkable properties in tyrosinase inhibition, anti-melanoma activity, and anti-migration effect. By furthering these studies, it will be possible to discover new compounds with anti-melanoma effects that inhibit tyrosinase.

### 4. Experimental

#### 4.1. Materials

In the synthesis and analytical studies, chemicals from Merck, Alfa Aesar, and Sigma-Aldrich were utilized. The STUART SMP40 and an Alfa



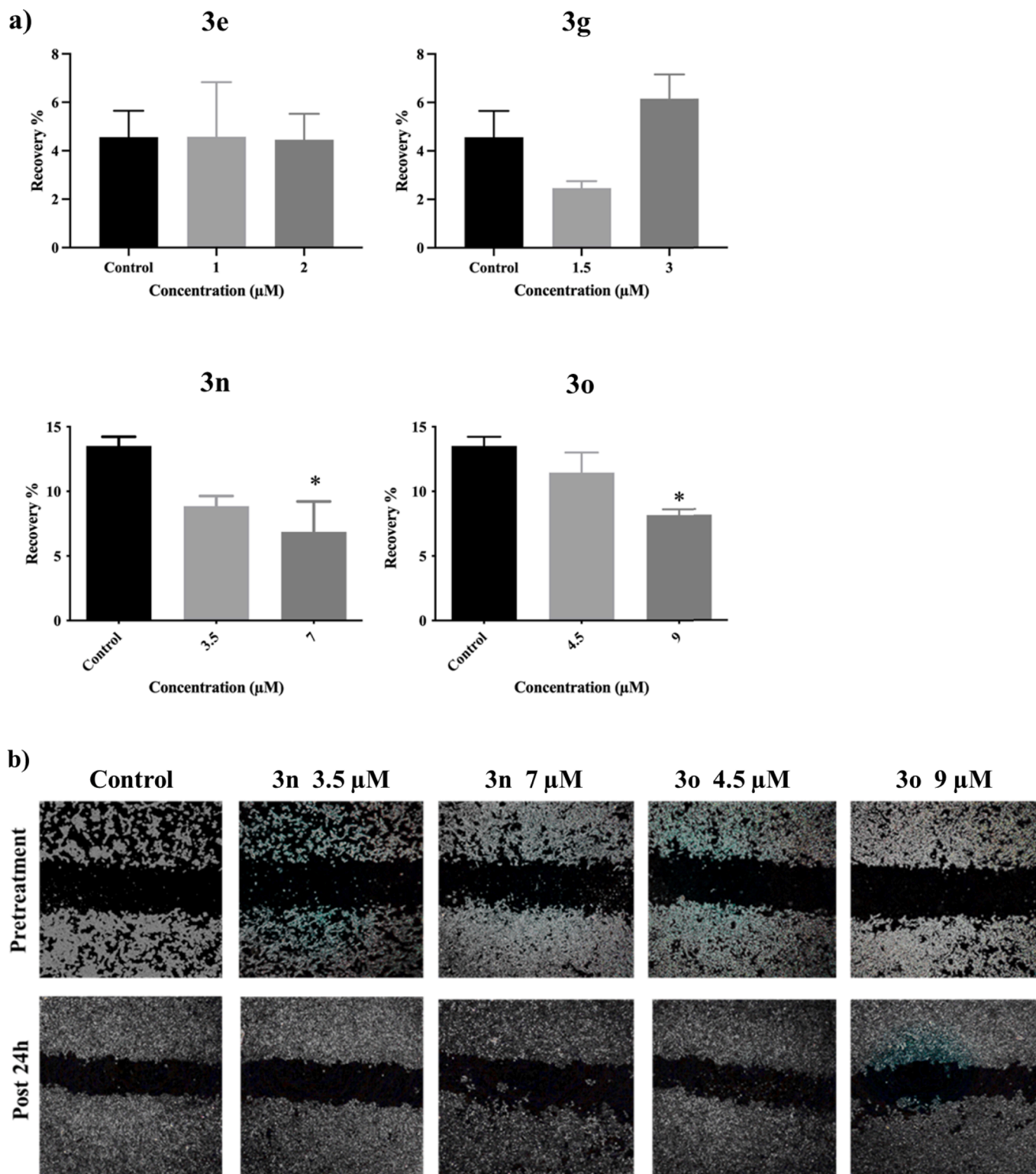


**Fig. 4.** a) Effects of **3e**, **3g**, **3n**, and **3o** on cell migration of B16F10 melanoma cells after 24 h treatment. b) Schematic representation of the closure of scratch due to cell migration after treatment with **3n** and **3o**. Data are expressed as mean  $\pm$  SD, \* $p < 0.05$  and \*\* $p < 0.01$  versus the control group.

Bruker spectrometer were used to determine the melting points and measure the IR spectra, respectively.  $^1\text{H}$  and  $^{13}\text{C}$  NMR spectra were assessed using a Varian spectrometer at 300 and 75 Hz, and a Bruker spectrometer at 500 and 125 Hz, respectively, while Mass spectra were collected using a Thermo Fisher Scientific LC-HRMS spectrometer. Biological activity experiments were spectrophotometrically analysed using a BioTek Powerwave XS (BioTek, USA). The American Type

Culture Collection (ATCC) provided the cell lines, used to assess the cytotoxicity of cells. Dulbecco's Modified Eagle's Medium-F12, RPMI Medium, fetal calf serum, and PBS were bought from GIBCO BRL, InVitrogen (Carlsbad, CA).

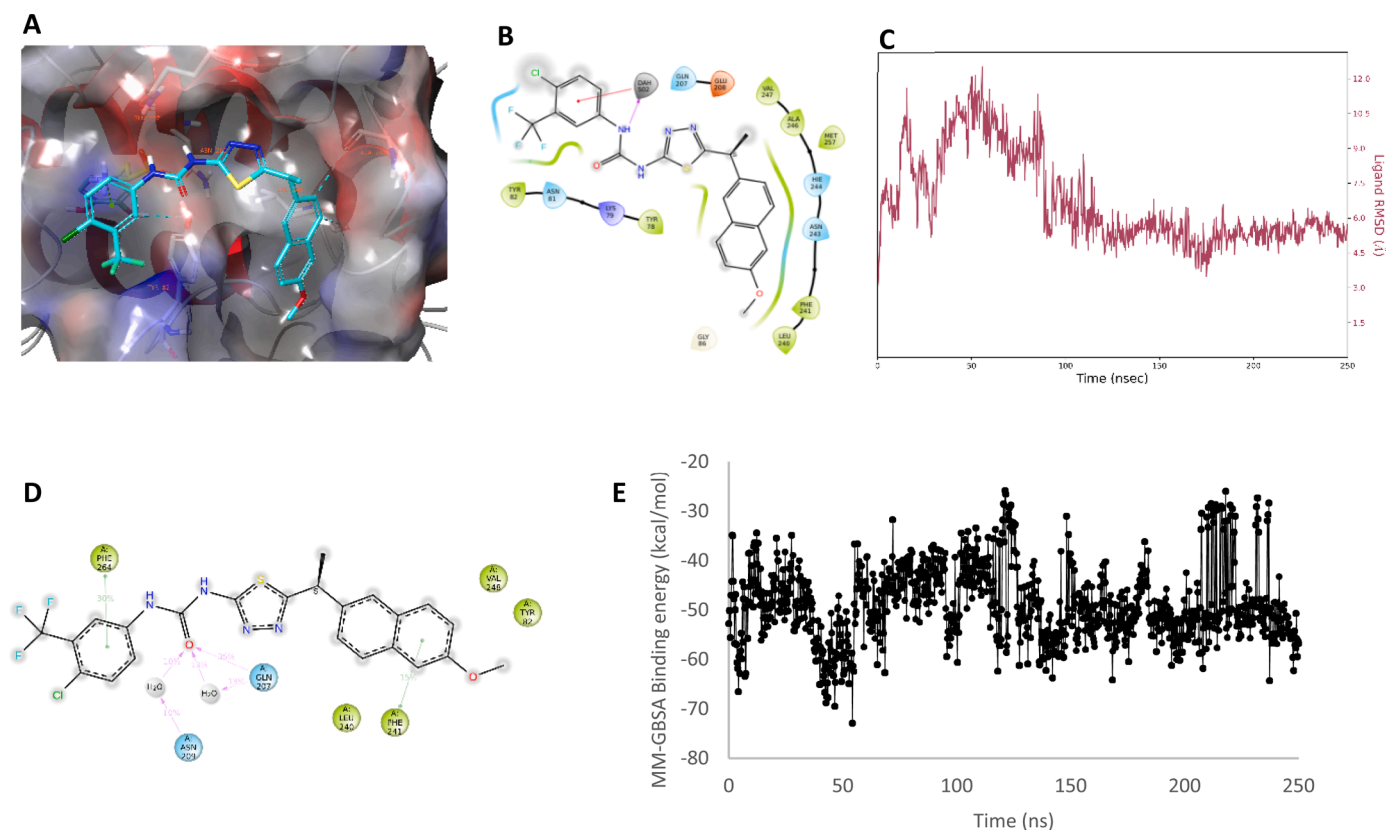


**Fig. 5.** Molecular modeling studies of the interactions of compound **3o** (turquoise) with the *Agaricus bisporus* Tyrosinase complexed with *L*-Tyrosine (green). The docked pose of compound **3o** in 3D and 2D view (A, B). The ligand RMSD value (C), the ligand-enzyme interactions (D) and MM-GBSA binding energy (E) during the 250 ns MD simulation.

## 4.2. Methods

### 4.2.1. General procedures and spectral data

#### 4.2.2. Synthesis of (S)-5-(1-(6-methoxynaphthalen-2-yl)ethyl)-1,3,4-thiadiazol-2-amine (2):

Naproxen (**1**) (2 mmol) and thiosemicarbazide (2 mmol) were dissolved in phosphorochloride (36 mmol) and this solution was stirred for 1 h at 75 °C, upon when it was poured into iced water. The mixture pH level was adjusted between 8–9 by the addition of a NaOH aqueous solution (50 %). The precipitates were filtered under vacuum, washed with water, and dried in a vacuum oven at 35 °C [30].

(S)-5-(1-(6-methoxynaphthalen-2-yl)ethyl)-1,3,4-thiadiazol-2-amine (**2**);  $^1\text{H NMR}$  (DMSO- $d_6$ , 300 MHz)  $\delta$ /ppm: 1.69 (3H, d,  $J = 7.0$  Hz), 4.61–4.52 (1H, m), 3.86 (3H, s), 7.14–7.21 (1H, m), 7.31 (1H, s), 7.41 (1H, d,  $J = 8.4$  Hz), 7.77–7.86 (4H, m), 8.72 (1H, s);  $^{13}\text{C NMR}$  (DMSO- $d_6$ , 75 MHz)  $\delta$ /ppm: 20.7, 55.6, 106.2, 119.4, 126.0, 126.5, 127.8, 128.8, 129.7, 133.9, 138.0, 157.8, 163.4, 169.5.

#### 4.2.3. Synthesis of naproxen thiadiazol-urea derivatives (3a–3p)

Compound **2** (0.60 mmol) and the corresponding phenyl isocyanates (0.66 mmol) were dissolved in 3 mL DMF in the presence of a catalytic amount of DBU. This mixture was stirred for 18 hours at 60 °C. After reaching room temperature, the mixture was poured into iced water and neutralized by the addition of HCl aqueous solution (5 %). The collected precipitates were filtered under vacuum, washed with water, and dried in a vacuum oven at 30 °C. The obtained naproxen thiadiazol-urea derivatives (**3a–3p**) were purified by column chromatography, using EtOAc/MeOH as eluent [31].

**4.2.3.1.** (S)-1-(3-fluorophenyl)-3-(5-(1-(6-methoxynaphthalen-2-yl)ethyl)-1,3,4-thiadiazol-2-yl)urea (**3a**) Pink powder, 73 % yield, 265 °C mp. IR: 3304, 3276, 3103, 2980, 2934, 1727, 1608, 1523, 1482, 1312,

1280, 1197, 1027, 872  $\text{cm}^{-1}$ ;  $^1\text{H NMR}$  (DMSO- $d_6$ , 300 MHz)  $\delta$ /ppm: 1.77 (3H, d,  $J = 7.3$  Hz), 3.87 (3H, s), 4.62–4.66 (1H, m), 6.80–6.85 (1H, m), 7.10–7.19 (2H, m), 7.26–7.34 (2H, m), 7.42–7.46 (2H, m), 7.75–7.84 (3H, m), 9.28 (1H, s);  $^{13}\text{C NMR}$  (DMSO- $d_6$ , 125 MHz)  $\delta$ /ppm: 21.0, 40.7, 55.6, 105.7, 105.9, 106.2, 109.5, 114.9, 119.3, 119.4, 125.9, 126.4, 126.6, 127.1, 127.8, 128.9, 129.7, 130.8, 130.9, 133.9, 138.7, 155.8, 157.7, 161.7, 163.7 ( $J_{\text{CF}} = 237.2$ ). HRMS (ESI)  $m/z$  calculated for  $\text{C}_{22}\text{H}_{19}\text{FN}_4\text{O}_2\text{S}$  [ $\text{M-H}$ ] $^-$ ; 421.1134, found: 421.1145.

**4.2.3.2.** (S)-1-(4-fluorophenyl)-3-(5-(1-(6-methoxynaphthalen-2-yl)ethyl)-1,3,4-thiadiazol-2-yl)urea (**3b**) White powder, 32 % yield, 220 °C mp. IR: 3374, 3102, 2871, 2768, 1718, 1600, 1549, 1450, 1307, 1269, 1028, 840  $\text{cm}^{-1}$ ;  $^1\text{H NMR}$  (DMSO- $d_6$ , 300 MHz)  $\delta$ /ppm: 1.80 (3H, d,  $J = 7.2$  Hz), 3.90 (3H, s), 4.68–4.70 (1H, m), 7.13–7.20 (3H, m), 7.22–7.35 (1H, m), 7.45–7.52 (3H, m), 7.83–7.87 (3H, m), 9.10 (1H, s);  $^{13}\text{C NMR}$  (DMSO- $d_6$ , 75 MHz)  $\delta$ /ppm: 21.3, 55.8, 106.4, 115.9, 116.2, 119.5, 121.2, 121.3, 126.1, 126.9, 127.9, 129.1, 129.9, 134.0, 135.6, 139.0, 157.9. HRMS (ESI)  $m/z$  calculated for  $\text{C}_{22}\text{H}_{19}\text{FN}_4\text{O}_2\text{S}$  [ $\text{M-H}$ ] $^-$ ; 421.1134, found: 421.1143.

**4.2.3.3.** (S)-1-(3-chlorophenyl)-3-(5-(1-(6-methoxynaphthalen-2-yl)ethyl)-1,3,4-thiadiazol-2-yl)urea (**3c**); Pink powder, 65 % yield, 252 °C mp. IR: 3370, 3103, 2935, 1714, 1590, 1447, 1289, 1088, 1029, 802  $\text{cm}^{-1}$ ;  $^1\text{H NMR}$  (DMSO- $d_6$ , 300 MHz)  $\delta$ /ppm: 1.76 (3H, d,  $J = 7.3$  Hz), 3.86 (3H, s), 4.64–4.66 (1H, m), 7.10–7.19 (1H, m), 7.30–7.33 (3H, m), 7.41–7.50 (3H, m), 7.74–7.84 (3H, m), 9.19 (1H, s);  $^{13}\text{C NMR}$  (DMSO- $d_6$ , 75 MHz)  $\delta$ /ppm: 21.2, 55.8, 106.4, 119.5, 120.9, 126.1, 126.8, 127.9, 128.0, 129.1, 129.3, 129.9, 134.1, 138.3, 138.9, 157.9. HRMS (ESI)  $m/z$  calculated for  $\text{C}_{22}\text{H}_{19}\text{ClN}_4\text{O}_2\text{S}$  [ $\text{M-H}$ ] $^-$ ; 437.0839, found: 437.0846.

**4.2.3.4.** (S)-1-(4-chlorophenyl)-3-(5-(1-(6-methoxynaphthalen-2-yl)ethyl)-1,3,4-thiadiazol-2-yl)urea (**3d**) White powder, 77 % yield, 255 °C mp. IR: 3371, 3120, 2935, 2769, 1714, 1590, 1539, 1446, 1309, 1291, 1088, 802  $\text{cm}^{-1}$ ;  $^1\text{H NMR}$  (DMSO- $d_6$ , 300 MHz)  $\delta$ /ppm: 1.77 (3H, d,

$J=6.7$  Hz), 3.87 (3H, s), 4.64–4.66 (1H, m), 7.12–7.19 (1H, m), 7.31–7.34 (3H, m), 7.42–7.52 (3H, m), 7.75–7.74 (3H, m), 9.22 (1H, s);  $^{13}\text{C}$  NMR (DMSO- $d_6$ , 75 MHz)  $\delta$ /ppm: 21.2, 55.8, 106.4, 119.5, 120.9, 126.1, 126.8, 127.0, 127.9, 129.1, 129.3, 129.9, 134.1, 138.4, 138.9, 157.9. HRMS (ESI)  $m/z$  calculated for  $\text{C}_{22}\text{H}_{19}\text{ClN}_4\text{O}_2\text{S}$  [M-H] $^+$ ; 437.0839, found: 437.0848.

**4.2.3.5.** (S)-1-(3,4-dichlorophenyl)-3-(5-(1-(6-methoxynaphthalen-2-yl)ethyl)-1,3,4-thiadiazol-2-yl)urea (**3e**) White powder, 48 % yield, 261°C mp. IR: 3365, 3102, 2932, 2739, 1718, 1584, 1476, 1381, 1207, 1030, 816  $\text{cm}^{-1}$ ;  $^1\text{H}$  NMR (DMSO- $d_6$ , 300 MHz)  $\delta$ /ppm: 1.73 (3H, d,  $J=7.0$  Hz), 3.87 (3H, s), 4.57–4.62 (1H, m), 7.14–7.21 (1H, m), 7.31 (1H, d,  $J=2.1$  Hz), 7.38–7.45 (2H, m), 7.48–7.54 (1H, m), 7.80–7.87 (4H, m), 9.40 (1H, s);  $^{13}\text{C}$  NMR (DMSO- $d_6$ , 75 MHz)  $\delta$ /ppm: 21.1, 55.8, 106.4, 119.4, 119.5, 120.4, 124.6, 126.2, 126.8, 128.0, 129.1, 129.9, 131.2, 131.7, 134.1, 138.8, 139.8, 158.0. HRMS (ESI)  $m/z$  calculated for  $\text{C}_{22}\text{H}_{18}\text{Cl}_2\text{N}_4\text{O}_2\text{S}$  [M-H] $^-$ ; 471.0449, found: 471.0457.

**4.2.3.6.** (S)-1-(4-iodophenyl)-3-(5-(1-(6-methoxynaphthalen-2-yl)ethyl)-1,3,4-thiadiazol-2-yl) urea (**3f**); White powder, 56 % yield, 217°C mp. IR: 3365, 3303, 3102, 2756, 1719, 1581, 1483, 1446, 1391, 1290, 1196, 1028, 854  $\text{cm}^{-1}$ ;  $^1\text{H}$  NMR (DMSO- $d_6$ , 300 MHz)  $\delta$ /ppm: 1.76 (3H, d,  $J=7.0$  Hz), 3.86 (3H, s), 4.61–4.68 (1H, m), 7.10–7.19 (1H, m), 7.28–7.31 (3H, m), 7.41–7.44 (1H, m), 7.58–7.74 (2H, m), 7.79–7.84 (3H, m), 9.13 (1H, s);  $^{13}\text{C}$  NMR (DMSO- $d_6$ , 75 MHz)  $\delta$ /ppm: 21.2, 55.8, 106.4, 119.5, 121.2, 121.6, 126.1, 126.9, 127.9, 129.1, 129.9, 134.1, 138.0, 158.0. HRMS (ESI)  $m/z$  calculated for  $\text{C}_{22}\text{H}_{19}\text{IN}_4\text{O}_2\text{S}$  [M-H] $^-$ ; 529.0195, found: 529.0203.

**4.2.3.7.** (S)-1-(5-(1-(6-methoxynaphthalen-2-yl)ethyl)-1,3,4-thiadiazol-2-yl)-3-phenylurea (**3g**) White powder, 62 % yield, 285°C mp. IR: 3302, 3146, 1724, 1523, 1309, 1179, 1045, 856, 751  $\text{cm}^{-1}$ ;  $^1\text{H}$  NMR (DMSO- $d_6$  500 MHz)  $\delta$ /ppm: 1.77 (3H, d,  $J=7.0$  Hz), 3.87 (3H, s), 4.63–4.70 (1H, m), 6.98–7.05 (1H, m), 7.14–7.20 (1H, m), 7.26–7.32 (3H, m), 7.42–7.46 (3H, m), 7.80–7.84 (3H, m), 9.03 (1H, s);  $^{13}\text{C}$  NMR (DMSO- $d_6$ , 75 MHz)  $\delta$ /ppm: 21.3, 55.8, 106.4, 119.3, 119.5, 123.5, 126.1, 126.9, 127.9, 129.1, 129.5, 129.9, 134.0, 139.0, 139.2, 157.9. HRMS (ESI)  $m/z$  calculated for  $\text{C}_{22}\text{H}_{20}\text{N}_4\text{O}_2\text{S}$  [M-H] $^-$ ; 403.1239, found: 403.1239.

**4.2.3.8.** (S)-1-(5-(1-(6-methoxynaphthalen-2-yl)ethyl)-1,3,4-thiadiazol-2-yl)-3-(p-tolyl)urea (**3h**) Pink powder, 42 % yield, 191.5°C mp. IR: 3376, 3103, 2870, 2765, 1716, 1595, 1509, 1449, 1313, 1202, 1029, 806  $\text{cm}^{-1}$ ;  $^1\text{H}$  NMR (DMSO- $d_6$ , 300 MHz)  $\delta$ /ppm: 1.77 (3H, d,  $J=7.1$  Hz), 2.23 (3H, s), 3.87 (3H, s), 4.61–4.64 (1H, m), 7.07–7.11 (2H, m), 7.14–7.20 (1H, m), 7.29–7.34 (3H, m), 7.41–7.46 (1H, m), 7.80–7.84 (3H, m), 8.88 (1H, s);  $^{13}\text{C}$  NMR (DMSO- $d_6$ , 75 MHz)  $\delta$ /ppm: 19.2, 21.0, 55.8, 106.4, 119.4, 119.5, 126.1, 126.8, 127.9, 129.1, 129.9, 132.5, 134.0, 136.5, 139.0, 157.9. HRMS (ESI)  $m/z$  calculated for  $\text{C}_{23}\text{H}_{22}\text{N}_4\text{O}_2\text{S}$  [M-H] $^-$ ; 417.1385, found: 417.1396.

**4.2.3.9.** (S)-1-(5-(1-(6-methoxynaphthalen-2-yl)ethyl)-1,3,4-thiadiazol-2-yl)-3-(3-methoxy phenyl) urea (**3i**); Pink powder, 52 % yield, 206.5°C mp. IR: 3375, 3102, 2960, 2934, 1712, 1596, 1454, 1302, 1260, 1195, 1027, 811  $\text{cm}^{-1}$ ;  $^1\text{H}$  NMR (DMSO- $d_6$ , 300 MHz)  $\delta$ /ppm: 1.81 (3H, d,  $J=6.8$  Hz), 3.74 (3H, s), 3.90 (3H, s), 4.64–4.74 (1H, m), 6.63 (1H, d,  $J=8.2$  Hz), 6.98 (1H, d,  $J=8.0$  Hz), 7.16–7.25 (3H, m), 7.35 (1H, s), 7.47 (1H, d,  $J=8.5$  Hz), 7.81–7.91 (3H, m), 9.08 (1H, s);  $^{13}\text{C}$  NMR (DMSO- $d_6$ , 75 MHz)  $\delta$ /ppm: 21.2, 55.6, 55.8, 104.9, 106.4, 109.0, 111.5, 119.5, 126.1, 126.9, 127.9, 129.1, 129.9, 130.3, 134.0, 139.0, 140.4, 157.9, 160.3. HRMS (ESI)  $m/z$  calculated for  $\text{C}_{23}\text{H}_{22}\text{N}_4\text{O}_3\text{S}$  [M-H] $^-$ ; 433.1334, found: 433.1344.

**4.2.3.10.** (S)-1-(5-(1-(6-methoxynaphthalen-2-yl)ethyl)-1,3,4-thiadiazol-2-yl)-3-(4-methoxy phenyl) urea (**3j**) White powder, 58 % yield, 257°C mp. IR: 3372, 3103, 2833, 1709, 1596, 1510, 1414, 1310, 1298, 1204, 1171, 1022, 852  $\text{cm}^{-1}$ ;  $^1\text{H}$  NMR (DMSO- $d_6$ , 300 MHz)  $\delta$ /ppm: 1.77 (3H, d,  $J=7.0$  Hz), 3.70 (3H, s), 3.87 (3H, s), 4.59–4.71 (1H, m), 6.82–6.90 (2H, m), 7.13–7.20 (1H, m), 7.30–7.35 (3H, m), 7.40–7.47 (1H, m), 7.78–7.85 (3H, m), 8.79 (1H, s);  $^{13}\text{C}$  NMR (DMSO- $d_6$ , 75 MHz)  $\delta$ /ppm: 21.3, 55.8, 106.4, 114.6, 119.5, 121.2, 126.1, 126.8, 127.9, 129.1, 129.9, 132.0, 134.0, 139.1, 155.8, 157.9. HRMS (ESI)  $m/z$

calculated for  $\text{C}_{23}\text{H}_{22}\text{N}_4\text{O}_3\text{S}$  [M-H] $^-$ ; 433.1334, found: 433.1344.

**4.2.3.11.** (S)-1-(5-(1-(6-methoxynaphthalen-2-yl)ethyl)-1,3,4-thiadiazol-2-yl)-3-(3-nitro phenyl) urea (**3k**); Yellow powder, 78 % yield, 232.2°C mp. IR: 3322, 3094, 2952, 1714, 1602, 1522, 1293, 1192, 1023, 737  $\text{cm}^{-1}$ ;  $^1\text{H}$  NMR (DMSO- $d_6$  500 MHz)  $\delta$ /ppm: 1.77 (3H, d,  $J=7.0$  Hz), 3.87 (3H, s), 4.61–4.70 (1H, m), 7.15–7.21 (1H, m), 7.32 (1H, d,  $J=1.6$  Hz), 7.45 (1H, d,  $J=8.5$  Hz), 7.55 (1H, t,  $J=8.1$  Hz), 7.73–7.90 (5H, m), 8.56 (1H, s), 9.72 (1H, s);  $^{13}\text{C}$  NMR (DMSO- $d_6$ , 125 MHz)  $\delta$ /ppm: 20.9, 55.6, 106.2, 113.0, 119.3, 125.1, 125.2, 126.0, 126.6, 127.8, 128.9, 129.7, 130.5, 133.9, 138.5, 148.5, 157.7. HRMS (ESI)  $m/z$  calculated for  $\text{C}_{22}\text{H}_{19}\text{N}_5\text{O}_4\text{S}$  [M-H] $^-$ ; 448.1079, found: 448.1091.

**4.2.3.12.** (S)-1-(5-(1-(6-methoxynaphthalen-2-yl)ethyl)-1,3,4-thiadiazol-2-yl)-3-(4-nitro phenyl) urea (**3l**); White powder, 77 % yield, 233°C mp. IR: 3320, 3060, 2950, 1712, 1552, 1200, 1103, 1026, 735  $\text{cm}^{-1}$ ;  $^1\text{H}$  NMR (DMSO- $d_6$  500 MHz)  $\delta$ /ppm: 1.81 (d,  $J=7.1$  Hz, 1H), 3.87 (s, 3H), 4.67 (d,  $J=7.1$  Hz, 3H), 7.17 (dd,  $J=8.9$ , 2.5 Hz, 1H), 7.32 (d,  $J=2.4$  Hz, 1H), 7.48 (dd,  $J=8.4$ , 1.6 Hz, 1H), 7.73 (d,  $J=9.2$  Hz, 1H), 7.86–7.80 (m, 3H), 7.97 (d,  $J=9.2$  Hz, 2H), 8.13 (d,  $J=9.3$  Hz, 2H), 8.21 (d,  $J=9.2$  Hz, 1H);  $^{13}\text{C}$  NMR (DMSO- $d_6$ , 125 MHz)  $\delta$ /ppm: 21.1, 55.6, 106.2, 109.0, 118.0, 118.4, 119.2, 125.4, 125.5, 125.9, 126.8, 127.6, 128.9, 129.7, 133.8, 139.0, 141.2, 141.9, 146.2, 147.4, 157.7, 165.8. HRMS (ESI)  $m/z$  calculated for  $\text{C}_{22}\text{H}_{19}\text{N}_5\text{O}_4\text{S}$  [M-H] $^-$ ; 448.1079, found: 448.1088.

**4.2.3.13.** (S)-1-(5-(1-(6-methoxynaphthalen-2-yl)ethyl)-1,3,4-thiadiazol-2-yl)-3-(3-(trifluoro methyl) phenyl)urea (**3m**); White powder, 65 % yield, 228°C mp. IR: 3374, 3096, 2900, 1704, 1600, 1490, 1280, 1160, 1020, 757  $\text{cm}^{-1}$ ;  $^1\text{H}$  NMR (DMSO- $d_6$  500 MHz)  $\delta$ /ppm: 1.77 (d,  $J=7.0$  Hz, 3H), 3.87 (s, 3H), 4.60–4.68 (m, 1H), 7.17 (dd,  $J=9.0$ , 2.4 Hz, 1H), 7.30–7.35 (m, 2H), 7.49–7.40 (m, 1H), 7.52 (d,  $J=7.9$  Hz, 1H), 7.71–7.62 (m, 1H), 7.98–7.84 (m, 3H), 7.99 (s, 1H), 9.63 (s, 1H);  $^{13}\text{C}$  NMR (DMSO- $d_6$ , 125 MHz)  $\delta$ /ppm: 21.1, 55.8, 106.4, 115.2, 115.3, 115.3, 119.5, 122.9, 126.1, 126.8, 128.0, 129.1, 129.9, 129.9, 130.6, 134.1, 138.8, 140.4, 157.9. HRMS (ESI)  $m/z$  calculated for  $\text{C}_{23}\text{H}_{19}\text{F}_3\text{N}_4\text{O}_2\text{S}$  [M-H] $^-$ ; 471.1103, found: 471.1108.

**4.2.3.14.** (S)-1-(5-(1-(6-methoxynaphthalen-2-yl)ethyl)-1,3,4-thiadiazol-2-yl)-3-(4-(trifluoro methyl) phenyl)urea (**3n**); White powder, 78 % yield, 237°C mp. IR: 3344, 3040, 2922, 1712, 1622, 1520, 1290, 1100, 1020, 735  $\text{cm}^{-1}$ ;  $^1\text{H}$  NMR (DMSO- $d_6$  500 MHz)  $\delta$ /ppm: 1.77 (d,  $J=5.9$  Hz, 3H), 4.66 (m, 1H), 3.87 (s, 3H), 7.18 (d,  $J=8.1$  Hz, 1H), 7.31 (s, 1H), 7.44 (d,  $J=7.7$  Hz, 1H), 7.63–7.70 (m, 4H), 7.78–7.84 (m, 3H), 9.52 (s, 1H);  $^{13}\text{C}$  NMR (DMSO- $d_6$ , 125 MHz)  $\delta$ /ppm: 21.0, 55.6, 106.2, 118.8, 119.3, 125.9, 126.5, 126.6, 127.8, 128.9, 129.7, 133.9, 138.6, 157.7. HRMS (ESI)  $m/z$  calculated for  $\text{C}_{23}\text{H}_{19}\text{F}_3\text{N}_4\text{O}_2\text{S}$  [M-H] $^-$ ; 471.1103, found: 471.1109.

**4.2.3.15.** (S)-1-(4-chloro-3-(trifluoromethyl)phenyl)-3-(5-(1-(6-methoxynaphthalen-2-yl)ethyl)-1,3,4-thiadiazol-2-yl)urea (**3o**); White powder, 67 % yield, 221°C mp. IR: 3336, 3080, 2932, 1708, 1600, 1500, 1280, 1100, 1004, 736  $\text{cm}^{-1}$ ;  $^1\text{H}$  NMR (DMSO- $d_6$  500 MHz)  $\delta$ /ppm: 1.76 (d,  $J=7.0$  Hz, 3H), 3.87 (s, 3H), 4.64 (q,  $J=6.6$  Hz, 1H), 7.18 (dd,  $J=8.9$ , 2.4 Hz, 1H), 7.32 (d,  $J=2.2$  Hz, 1H), 7.44 (dd,  $J=8.4$ , 1.5 Hz, 1H), 7.61 (d,  $J=8.8$  Hz, 1H), 7.72 (d,  $J=8.1$  Hz, 1H), 7.80–7.84 (m, 3H), 8.12 (s, 1H), 9.63 (s, 1H);  $^{13}\text{C}$  NMR (DMSO- $d_6$ , 125 MHz)  $\delta$ /ppm: 20.8, 40.8, 55.6, 106.2, 117.7, 119.3, 122.1, 123.9, 124.2 ( $J_{\text{CF}}^1=176.2$ ), 126.0, 126.6, 127.0, 127.2, 127.8, 128.9, 129.7, 132.4, 133.9, 138.5, 157.8. HRMS (ESI)  $m/z$  calculated for  $\text{C}_{23}\text{H}_{18}\text{ClF}_3\text{N}_4\text{O}_2\text{S}$  [M-H] $^-$ ; 505.0713, found: 505.0721.

**4.2.3.16.** (S)-1-(5-(1-(6-methoxynaphthalen-2-yl)ethyl)-1,3,4-thiadiazol-2-yl)-3-(naphthalen-1-yl)urea (**3p**); White powder, 82 % yield, 197°C mp. IR: 3300, 3024, 2940, 1710, 1604 1556, 1266, 1190, 1020, 757  $\text{cm}^{-1}$ ;  $^1\text{H}$  NMR (DMSO- $d_6$  500 MHz)  $\delta$ /ppm: 1.79 (d,  $J=6.7$  Hz, 3H), 3.86 (s, 3H), 4.69 (d,  $J=6.6$  Hz, 1H), 7.17 (d,  $J=8.4$  Hz, 1H), 7.31 (s, 1H), 7.43–7.48 (m, 2H), 7.58 (d,  $J=6.6$  Hz, 2H), 7.71 (d,  $J=8.0$  Hz, 1H), 7.87–7.77 (m, 3H), 7.90 (d,  $J=6.7$  Hz, 1H), 7.95 (d,  $J=7.8$  Hz, 1H), 8.04 (s, 1H), 9.11 (s, 1H), 11.15 (s, 1H);  $^{13}\text{C}$  NMR (DMSO- $d_6$ , 125 MHz)  $\delta$ /ppm: 21.2, 55.6, 106.2, 119.3, 121.6, 124.7, 125.9, 126.2, 126.5, 126.6, 126.7, 127.7, 128.9, 129.7, 133.8, 134.1, 138.9, 157.7.

HRMS (ESI)  $m/z$  calculated for  $C_{26}H_{22}N_4O_2S$   $[M-H]^-$ ; 453.1385, found: 453.1396.

#### 4.3. Tyrosinase inhibition assays

In the enzyme activity and inhibition studies, mushroom (*Agaricus bisporus*) tyrosinase was used because of its similarity to human tyrosinase [32,33]. Tyrosinase activity was measured spectrophotometrically at 492 nm using *L*-DOPA as a substrate [34]. One unit (U) tyrosinase activity was defined as 1  $\mu$ M of product, formed in 1 mL of mixture for 1 min [35]. The synthesized compounds were dissolved in DMF and solutions of different concentrations were prepared. Inhibition studies were carried out with 2 % solvent in the reaction medium. The  $IC_{50}$  values were calculated by drawing the graph of the inhibitory concentration versus the relative activity %. The type of inhibition was determined from the Lineweaver-Burk plot drawn for the **3o** with the best  $IC_{50}$  value and choosing two of the inhibitor concentrations in the range of 25–75 % (ISBN: 978-0-471-35,929-6). The  $K_i$  value was calculated from the Lineweaver-Burk graph. Kinetic studies were calculated using the following equation [36].

$$v = (V_{\max}S)/(1 + K_m/S + I/K_i)$$

#### 4.4. Cytotoxicity assay

The cytotoxicity of the test compounds on B16F10 murine melanoma cell line and 3T3 mouse embryonic cell line were evaluated according to the MTT (3-(4,5 dimethylthiazol-2-yl)-2,5- diphenyltetrazolium bromide) method [37].

#### 4.5. Cell migration

For evaluating the migration of the B16F10 melanoma cells the CytoSelect 24-well Wound Healing Assay Kit (Cell Biolabs Inc, USA) was used. The inserts were placed inside every well of the 24 well plate using a sterile forceps with their “wound field” aligned in the same direction. 500  $\mu$ L of medium containing  $2 \times 10^5$  cells was added to the gaps of the inserts. After 24 h incubation in a cell culture incubator overnight for the cells to provide a monolayer, the inserts were removed, and the images of each well were taken before treatment. **3e**, **3 g**, **3n**, and **3o** were studied for their anti-migration potential and their concentrations were determined according to the  $IC_{50}$  values of the cytotoxicity assay (2.17  $\mu$ M, 3.43  $\mu$ M, 7.41  $\mu$ M, 9.57  $\mu$ M, respectively). After taking the pre-treatment images, treatments were done in triplicate and the images of the same area of the wounds were taken after 24 h treatment. For analysing the cell migration percentage, the program ImageJ (National Institutes of Health, USA) was used, and comparison was done between the treatment groups vs. the control group (untreated cells).

#### 4.6. Molecular modeling studies

The Schrödinger software package (v2022-4, Schrödinger, Inc., New York) was used for the molecular modeling studies.

##### 4.6.1. Homology modeling and preparation of protein models for docking studies

Using the Prime tool, a homology model of *Agaricus bisporus* Tyrosinase (UniProt entry: C7FF04) was constructed based on the crystal structure of *Aspergillus oryzae* Tyrosinase in complex with *L*-tyrosine (PDB entry: 6JU9; chain A). The overall sequence identity was 34 %, while the sequence identity for the active site residues was 74 %. The active site Copper ions, which have shown to preserve enzyme activity, and the cocrystallized *L*-Tyrosine were incorporated into the homology model building procedure. The Protein Preparation Wizard module was used to prepare the homology model. The N- and C-terminals of the proteins were capped and subsequently, the system was minimized using the OPLS4 force field.

#### 4.6.2. Docking studies

Grid files were generated for the active site using the Receptor Grid Generation tool. All hydroxyl groups of the Ser, Thr and Tyr residues that were lining the binding pocket were allowed to rotate during dockings.

The three-dimensional structure of compound **3o** was prepared with the Builder and LigPrep tools. Both stereoisomers were generated. Subsequently, compound **3o** was docked into the active site using the Glide tool and Standard Precision (SP) scoring function with default settings. The highest scoring three poses were retained and investigated for complementarity in shape, hydrogen bonding characteristics, electrostatics and hydrophobicity between ligand and binding pocket.

#### 4.6.3. Molecular dynamics simulations

As we clearly stated in our previous publication, all molecular dynamics simulations were performed using the Desmond tool [38].

#### 4.7. Statistical analysis

Statistical analysis was performed using Graphpad Prism 9. Statistical differences were evaluated with one-way ANOVA followed by the Tukey test. The results were represented as mean  $\pm$  standard deviation (SD).

#### Support Information

The  $^1H$ ,  $^{13}C$  NMR and MS spectra of synthesized compounds and viability (%)–log concentration ( $\mu$ M) curves for the cytotoxic effects and  $IC_{50}$  curves of tyrosinase inhibition are given in Support Information.

#### CRediT authorship contribution statement

**Belma Zengin Kurt:** Conceptualization, Funding acquisition, Investigation, Methodology, Project administration, Visualization, Writing – original draft, Writing – review & editing. **Özlem Altundağ:** Methodology. **Mustafa Gökçe:** Methodology. **Ummuhan Cakmak:** Methodology. **Fulya Oz Tuncay:** Methodology. **Yakup Kolcuoğlu:** Methodology, Visualization, Writing – original draft, Writing – review & editing. **Ayşenur Günaydın Akyıldız:** Methodology, Visualization, Writing – original draft. **Atilla Akdemir:** Methodology, Visualization, Writing – original draft. **Dilek Öztürk Civelek:** Methodology, Visualization, Writing – original draft. **Fatih Sönmez:** Visualization, Writing – original draft, Writing – review & editing.

#### Declaration of Competing Interest

The authors declare that they have no known competing financial interests or personal relationships that could have appeared to influence the work reported in this paper.

#### Data availability

No data was used for the research described in the article.

#### Acknowledgments

This work was supported by the Bezmialem Research Fund of the Bezmialem Vakıf University. Project Number: 12.2017/31.

#### Supplementary materials

Supplementary material associated with this article can be found, in the online version, at [doi:10.1016/j.molstruc.2023.136618](https://doi.org/10.1016/j.molstruc.2023.136618).



## References

- [1] J. Li, L. Feng, L. Liu, F. Wang, L. Ouyang, L. Zhang, X.Y. Hu, G. Wang, Recent advances in the design and discovery of synthetic tyrosinase inhibitors, *Eur. J. Med. Chem.* 224 (2021).
- [2] N. Gencer, D. Demir, F. Sonmez, M. Kucukislamoglu, New saccharin derivatives as tyrosinase inhibitors, *Bioorg. Med. Chem.* 20 (9) (2012) 2811–2821.
- [3] K. Haldys, W. Goldeman, M. Jewginski, E. Wolinska, N. Anger, J. Rossowska, R. Latajka, Inhibitory properties of aromatic thiosemicarbazones on mushroom tyrosinase: Synthesis, kinetic studies, molecular docking and effectiveness in melanogenesis inhibition, *Bioorg. Chem.* 81 (2018) 577–586.
- [4] M. Ashooriha, M. Khoshneviszadeh, M. Khoshneviszadeh, A. Rafiei, M. Kardan, R. Yazdian-Robati, S. Emami, Kojic acid-natural product conjugates as mushroom tyrosinase inhibitors, *Eur. J. Med. Chem.* 201 (2020).
- [5] S. Ullan, C. Park, M. Ikram, D. Kang, S. Lee, J. Yang, Y. Park, S. Yoon, P. Chun, H. R. Moon, Tyrosinase inhibition and anti-melanin generation effect of cinnamide analogues, *Bioorg. Chem.* 87 (2019) 1255–1264.
- [6] S.C. Song, A. You, Z.Y. Chen, G.X. Zhu, H. Wen, H.C. Song, W. Yi, Study on the design, synthesis and structure-activity relationships of new thiosemicarbazone compounds as tyrosinase inhibitors, *Eur. J. Med. Chem.* 139 (2017) 815–825.
- [7] H.J. Jung, S.G. Noh, Y. Park, D. Kang, P. Chun, H.Y. Chung, H.R. Moon, In vitro and in silico insights into tyrosinase inhibitors with (E)-benzylidene-1-indanone derivatives, *Comput. Struct. Biotech.* 17 (2019) 1255–1264.
- [8] H. Hosseinpour, S.M. Farid, A. Iraj, S. Askari, N. Edraki, S. Hosseini, A. Jamshidzadeh, B. Larijani, M. Attaroshan, S. Pirhadi, M. Mahdavi, M. Khoshneviszadeh, Anti-melanogenesis and anti-tyrosinase properties of aryl-substituted acetamides of phenoxy methyl triazole conjugated with thiosemicarbazide: Design, synthesis and biological evaluations, *Bioorg. Chem.* 114 (2021).
- [9] L. Ielo, B. Deri, M.P. Germano, S. Vittorio, S. Mirabile, R. Gitto, A. Rapisarda, S. Ronsisvalle, S. Floris, Y. Pazy, A. Fais, A. Fishman, L. De Luca, Exploiting the 1-(4-fluorobenzyl)piperazine fragment for the development of novel tyrosinase inhibitors as anti-melanogenic agents: Design, synthesis, structural insights and biological profile, *Eur. J. Med. Chem.* 178 (2019) 380–389.
- [10] R. Romagnoli, P. Oliva, F. Prencipe, S. Manfredini, F. Ricci, D. Corallo, S. Aveic, E. Mariotto, G. Viola, R. Bortolozzi, M.P. Germano, L. De Luca, Cinnamic acid derivatives linked to arylpiperazines as novel potent inhibitors of tyrosinase activity and melanin synthesis, *Eur. J. Med. Chem.* 231 (2022).
- [11] N. Alizadeh, M.H. Sayahi, A. Iraj, R. Yazaf, A. Moazzam, K. Mobaraki, M. Adib, M. Attaroshan, B. Larijani, H. Rastegar, M. Khoshneviszadeh, M. Mahdavi, Evaluating the effects of disubstituted 3-hydroxy-1H-pyrrol-2(5H)-one analog as novel tyrosinase inhibitors, *Bioorg. Chem.* 126 (2022).
- [12] K. Piechowska, M. Switalska, J. Cytarska, K. Jaroch, K. Luczykowski, J. Chalupka, J. Wietrzyk, K. Misiura, B. Bojko, S. Kruszewski, K.Z. Laczkowski, Discovery of tropinone-thiazole derivatives as potent caspase 3/7 activators, and noncompetitive tyrosinase inhibitors with high antiproliferative activity: Rational design, one-pot tricomponent synthesis, and lipophilicity determination, *Eur. J. Med. Chem.* 175 (2019) 162–171.
- [13] K. Tang, Y. Jiang, H.W. Zhang, W.L. Huang, Y.D. Xie, C. Deng, H.B. Xu, X.M. Song, H. Xu, Design, synthesis of Cinnamyl-paeonol derivatives with 1, 3-Dioxypropyl as link arm and screening of tyrosinase inhibition activity in vitro, *Bioorg. Chem.* 106 (2021).
- [14] M.T. Varela, M. Ferrarini, V.G. Mercaldi, B.D. Sufi, G. Padovani, L.L.S. Nazato, J.P. S. Fernandes, Coumaric acid derivatives as tyrosinase inhibitors: Efficacy studies through in silico, in vitro and ex vivo approaches, *Bioorg. Chem.* 103 (2020).
- [15] S.Y. Seo, V.K. Sharma, N. Sharma, Mushroom tyrosinase: Recent prospects, *J. Agr. Food Chem.* 51 (10) (2003) 2837–2853.
- [16] F.A. Larik, A. Saeed, P.A. Channar, U. Muqadar, Q. Abbas, M. Hassan, S.Y. Seo, M. Bolte, Design, synthesis, kinetic mechanism and molecular docking studies of novel 1-pentanoyl-3-arylthioureas as inhibitors of mushroom tyrosinase and free radical scavengers, *Eur. J. Med. Chem.* 141 (2017) 273–281.
- [17] A. Mrozek-Wilczkiewicz, K. Malarz, M. Rejmund, J. Polanski, R. Musiol, Anticancer activity of the thiosemicarbazones that are based on di-2-pyridine ketone and quinoline moiety, *Eur. J. Med. Chem.* 171 (2019) 180–194.
- [18] D.L. Sun, S. Poddar, R.D. Pan, E.W. Rosser, E.R. Abt, J. Van Valkenburgh, T.M. Le, V. Lok, S.P. Hernandez, J. Song, J. Li, A. Turlik, X.H. Chen, C.A. Cheng, W. Chen, C. E. Mona, A.D. Stuparu, L. Vergnes, K. Reue, R. Damoiseaux, J.I. Zink, J. Czernin, T. R. Donahue, K.N. Houk, M.E. Jung, C.G. Radu, Isoquinoline thiosemicarbazone displays potent anticancer activity with in vivo efficacy against aggressive leukemias, *Rsc. Med. Chem.* 11 (3) (2020) 392–410.
- [19] R.B. de Oliveira, E.M. de Souza-Fagundes, R.P.P. Soares, A.A. Andrade, A.U. Kretzli, C.L. Zani, Synthesis and antimicrobial activity of semicarbazone and thiosemicarbazone derivatives, *Eur. J. Med. Chem.* 43 (9) (2008) 1983–1988.
- [20] R. Matsa, P. Makam, M. Kaushik, S.L. Hoti, T. Kannan, Thiosemicarbazone derivatives: Design, synthesis and in vitro antimicrobial activity studies, *Eur. J. Pharm. Sci.* 137 (2019).
- [21] A. Ezzat, M.B.I. Mohamed, A.M. Mahmoud, R.S. Farag, A.S. El-Tabl, A. Ragab, Synthesis, spectral characterization, antimicrobial evaluation and molecular docking studies of new Cu (II), Zn (II) thiosemicarbazone based on sulfonyl isatin, *J. Mol. Struct.* (2022) 1251.
- [22] K. Haldys, W. Goldeman, M. Jewginski, E. Wolinska, N. Anger-Gora, J. Rossowska, R. Latajka, Halogenated aromatic thiosemicarbazones as potent inhibitors of tyrosinase and melanogenesis, *Bioorg. Chem.* 94 (2020).
- [23] A.S.A.-B. Faisal, M. Aqlan, N.F. Alqahtani, M.Y. Wani, S.A. Khan, Thiazolidinone: A structural motif of great synthetic and biological importance, *J. Mol. Struct.* 1250 (2022), 131771.
- [24] A.M. Gouda, E.A. Beshr, F.A. Almalki, H.H. Halawan, B.F. Taj, A.F. Alnafeei, R. S. Alharazi, W.M. Kazi, M.M. AlMatrafi, Arylpropionic acid-derived NSAIDs: New insights on derivatization, anticancer activity and potential mechanism of action, *Bioorg. Chem.* 92 (2019).
- [25] W.R. Waddell, G.F. Ganser, E.J. Cerise, R.W. Loughry, Sulindac for polyposis of the colon, *Am. J. Surg.* 157 (1) (1989) 175–179.
- [26] K. Okamoto, Y. Saito, K. Narumi, A. Furugen, K. Iseki, M. Kobayashi, Anticancer effects of non-steroidal anti-inflammatory drugs against cancer cells and cancer stem cells, *Toxicol. In Vitro* 74 (2021).
- [27] H.Y. Kang, Y.M. Choi, FK506 increases pigmentation and migration of human melanocytes, *Brit. J. Dermatol.* 155 (5) (2006) 1037–1040.
- [28] C. Niu, H.A. Aisa, Upregulation of melanogenesis and tyrosinase activity: potential agents for vitiligo, *Molecules* 22 (8) (2017).
- [29] S. Jeon, N.H. Kim, B.S. Koo, H.J. Lee, A.Y. Lee, Bee venom stimulates human melanocyte proliferation, melanogenesis, dendricity and migration, *Exp. Mol. Med.* 39 (5) (2007) 603–613.
- [30] R. Ujan, A. Saeed, P.A. Channar, F.A. Larik, Q. Abbas, M.F. Alajmi, H.R. El-Seedi, M.A. Rind, M. Hassan, H. Raza, S.Y. Seo, Drug-1,3,4-thiadiazole conjugates as novel mixed-type inhibitors of acetylcholinesterase: synthesis, molecular docking, pharmacokinetics, and ADMET evaluation, *Molecules* 24 (5) (2019).
- [31] B.Z. Kurt, I. Gazioglu, F. Sonmez, M. Kucukislamoglu, Synthesis, antioxidant and anticholinesterase activities of novel coumarylthiazole derivatives, *Bioorg. Chem.* 59 (2015) 80–90.
- [32] X. Tan, Y.H. Song, C. Park, K.W. Lee, J.Y. Kim, D.W. Kim, K.D. Kim, K.W. Lee, M. J. Curtis-Long, K.H. Park, Highly potent tyrosinase inhibitor, neorauflavone from *Campylopus hirtella* and inhibitory mechanism with molecular docking, *Bioorg. Med. Chem.* 24 (2) (2016) 153–159.
- [33] J. Choi, S.J. Park, J.G. Jee, Analogues of ethionamide, a drug used for multidrug-resistant tuberculosis, exhibit potent inhibition of tyrosinase, *Eur. J. Med. Chem.* 106 (2015) 157–166.
- [34] G. Karakaya, A. Ture, A. Ercan, S. Oncul, M.D. Aytemir, Synthesis, computational molecular docking analysis and effectiveness on tyrosinase inhibition of kojic acid derivatives, *Bioorg. Chem.* 88 (2019).
- [35] Y. Kolcuoglu, I. Kuyumcu, A. Colak, A catecholase from *Laccaria laccata* a wild edible mushroom and its catalytic efficiency in organic media, *J. Food Biochem.* 42 (5) (2018).
- [36] X. Lv, R. Bai, J.K. Yan, H.L. Huang, X.K. Huo, X.G. Tian, X.Y. Zhao, B.J. Zhang, W. Y. Zhao, C.P. Sun, Investigation of the inhibitory effect of protostanes on human carboxylesterase 2 and their interaction: Inhibition kinetics and molecular stimulations, *Int. J. Biol. Macromol.* 167 (2021) 1262–1272.
- [37] B. Zengin Kurt, F. Sonmez, D. Ozturk, A. Akdemir, A. Angeli, C.T. Supuran, Synthesis of coumarin-sulfonamide derivatives and determination of their cytotoxicity, carbonic anhydrase inhibitory and molecular docking studies, *Eur. J. Med. Chem.* 183 (2019), 111702.
- [38] M. Trawally, K. Demir-Yazici, S.I. Dings-Birgöl, K. Kaya, A. Akdemir, Ö. Güzel-Akdemir, Dithiocarbamates and dithiocarbonates containing 6-nitrosaccharin scaffold: Synthesis, antimycobacterial activity and in silico target prediction using ensemble docking-based reverse virtual screening, *J. Mol. Struct.* 1277 (2023), 134818.